



Contents lists available at ScienceDirect

European Journal of Medicinal Chemistry

journal homepage: <http://www.elsevier.com/locate/ejmech>

Research paper

Identification of SENP1 inhibitors through *in silico* screening and rational drug design

Yaxue Zhao, Zhongli Wang, Jianchen Zhang, Huchen Zhou*

State Key Laboratory of Microbial Metabolism, School of Pharmacy, Shanghai Jiao Tong University, Shanghai 200240, People's Republic of China

ARTICLE INFO

Article history:

Received 25 March 2016

Received in revised form

11 June 2016

Accepted 11 June 2016

Available online 14 June 2016

Keywords:

SENP1 inhibitor

In silico screening

Rational design

Cancer

ABSTRACT

The small ubiquitin-related modifier (SUMO)-specific proteases (SENPs) catalyze the deconjugation of SUMO from their substrate proteins. SENP1 which is the most studied isoform is closely related to many cancers such as prostate cancer and colon cancer, thus representing a potential therapeutic target for cancer treatment. In the present study, we identified eleven SENP1 inhibitors representing a variety of scaffolds through *in silico* screening. Based on these scaffolds, a series of new compounds were designed and synthesized in order to improve their SENP1 inhibitory potency. As a result, compounds with IC₅₀ as low as 3.5 μM (compound **13m**) were obtained and a preliminary structure-activity relationship was discussed.

© 2016 Elsevier Masson SAS. All rights reserved.

1. Introduction

Small ubiquitin-like modifier (SUMO) is a member of the ubiquitin-like protein family that modulates cellular functions of a variety of target proteins [1–3]. Sumoylation has emerged as an important protein post-translational modification that can participate in transcriptional regulation, nuclear transport, maintenance of genome integrity, and signal transduction in human [4,5]. Dysfunction of sumoylation is associated with a broad range of diseases including cancer, neurodegenerative syndrome, diabetes, viral infection, and development defects [6]. As a reversible process, sumoylation is mediated by SUMO-activating enzyme (E1), SUMO-conjugation enzyme (E2) and SUMO protein ligase (E3), and is readily reversed by a family of SUMO-specific proteases (SENPs) [7]. SENPs, a family of cysteine proteases are responsible for the deconjugation of SUMO from substrate proteins [8]. Six isoforms of SENPs (SENP1, 2, 3, 5, 6, and 7) from human have been identified and characterized, each of them has a distinct subcellular localization and substrate specificity [9,10]. Among them, SENP1 has

been shown to be overexpressed in more than 50% of prostate cancer, and the critical role of SENP1 in tumorigenesis has been demonstrated in transgenic mice [11–13]. Furthermore, it has been found that SENP1 is essential for colon cancer cell growth [14], and enhances vascular endothelial growth factor (VEGF) production by regulating the stability of hypoxia-inducible factor-1 (HIF-1) [15,16]. Thus, SENP1 may serve as an attractive target for developing new cancer therapeutics.

Since 2011, several SENP1 inhibitors have been reported by our and other groups [17–20], including the benzodiazepine-based peptidomimetic covalent inhibitors from our group [17], the SUMO-derived peptide-based covalent inhibitors from Bogyo's group [18], the 2-(4-chlorophenyl)-2-oxoethyl 4-benzamidobenzoates and 1-[4-(*N*-benzylamino)phenyl]-3-phenylureas as non-covalent inhibitors from Zhang [19] and Chen's [20] groups, respectively. These inhibitors showed moderate inhibitory activity which needs major improvement in order to be useful for in-depth *in vivo* studies. At the same time, the availability of a variety of scaffolds would also facilitate the discovery of potent inhibitors, and eventually lead to the development of therapeutic agents for SENP1-related pathological conditions and chemical probes to further the understanding of the biological functions of SENP1.

In this study, we identified a number of new scaffolds as SENP1 inhibitors through *in silico* screening. Two of the scaffolds were analyzed and a hybrid structure based on these two scaffolds was designed and optimized by structure-based rational design. Thus, a

Abbreviations: SUMO, small ubiquitin-related modifier; SENP, SUMO-specific protease; pre-SUMO, SUMO precursor; E1, SUMO-activating enzyme; E2, SUMO-conjugation enzyme; E3, SUMO protein ligase; VEGF, vascular endothelial growth factor; HIF1, hypoxia-inducible factor 1; HTVS, high-throughput virtual screening; SP, standard precision; XP, extra precision.

* Corresponding author.

E-mail address: hczhou@sjtu.edu.cn (H. Zhou).

series of new SENP1 inhibitors were developed and an IC₅₀ value as low as 3.5 μM (compound **13m**) was achieved. This work demonstrated that *in silico* screening followed with rational design is an effective strategy for the discovery of inhibitors against novel targets such as SENP1. It also provided new lead compounds for further development of SENP1 inhibitors as potential therapeutic agents and functional probes.

2. Results and discussion

2.1. Inhibitor identification via *in silico* screening

The SENP1 protein undergoes significant conformational change upon substrate protein binding and a binding tunnel capped by residues Trp465 and Val532 is induced. Thus, the co-crystal structure of SENP1 and pre-SUMO [21] (PDB ID: 2IY1) was used as the starting structure for *in silico* screening as it represents the binding conformation of SENP1 with the presence of the binding tunnel (Fig. 1A).

The catalytic triad, Cys603, His533, and Asp550, of SENP1 is critical for its catalytic activity, the corresponding mutants (C603A, H533A, and D550A) are completely inactive in the deconjugation of SUMO [22]. The binding tunnel of SENP1, which is composed of amino acids Trp465, His529, Val532, Trp534, and Leu466, is essential for interactions with the C-terminal of SUMO for the subsequent deconjugation of SUMO from modified proteins. The catalytic activity of SENP1 is seriously impaired or completely abolished in the corresponding mutants including W465A, H529A, and W534A [22]. Thus, these key residues, Trp465, Leu466, His529, Val532, His533, Trp534 and Cys603, are all included in the docking box (Fig. 1A) for virtual screening. The centroid of T⁹⁰GGH⁹³ peptide (red in Fig. 1A) located inside the binding tunnel is used to generate the docking grid.

As shown in Fig. 1B, the compounds from Specs database were prepared by LigPrep and screened by Glide in three consecutive modes: high-throughput virtual screening (HTVS), standard precision (SP), and extra precision (XP). The top ranked 150 molecules from SP screening and the top ranked 150 molecules from XP screening were submitted to manual inspection using the following

criteria: binding pose should closely resemble that of pre-SUMO, at least four hydrogen bonds should be formed, and scaffold diversity should be considered. Finally, 30 compounds were selected and purchased for SENP1 inhibitory assay.

We showed that 11 of the 30 selected compounds showed SENP1 inhibitory activities with IC₅₀ below 50 μM (Table 1). These inhibitors represent a diversity of scaffolds, providing hits for further optimization and development (see Table 2).

2.2. Representative structures of SENP1 inhibitors

Among the identified SENP1 inhibitors with IC₅₀ values below 20 μM, the structures of compounds **1**, **5**, **7** and **9** can be summarized into a representative structure, A¹-L¹-A²-L²-A³, as shown in Fig. 2A. In the docked poses, the A¹ moiety points to either the Phe496-His529 site or the Lys455-Thr459-Asn467-Asp468 site. The L¹-A²-L² moiety is inserted into the binding tunnel and covered by residues Trp465, Leu466, His529, Val532, Trp534, Gln597, and Cys603. The A² moiety has conserved interaction with Trp465 and/

Table 1
Inhibitory effect of hit compounds from *in silico* screening against SENP1.

Compound	Structure	IC ₅₀ ^a (μM)
1		15.0
2		20.7
3		28.4
4		14.0
5		17.6
6		47.9
7		15.8
8		20.8
9		18.4
10		23.5
11		21.2

^a IC₅₀ measurement has an error range within ±10%.

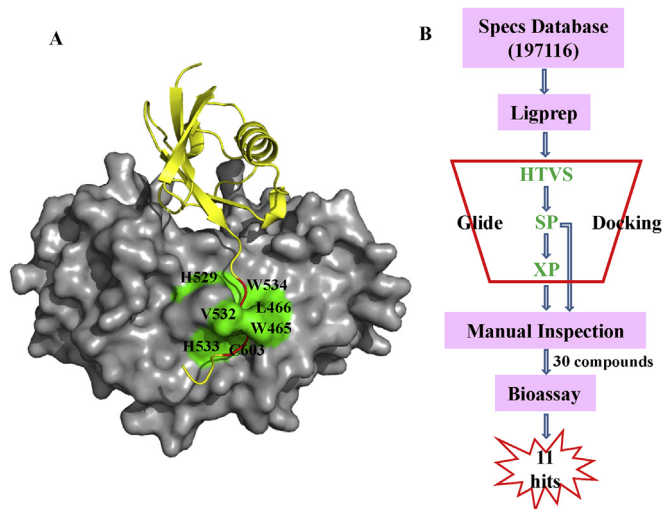


Fig. 1. A, Complex of SENP1 (gray surface) and pre-SUMO (yellow cartoon) (PDB ID: 2IY1). The key residues of SENP1 are shown in green, the T⁹⁰GGH⁹³ peptide of pre-SUMO which is used for docking box definition is shown in red. B, Schematic representation of our hit discovery strategy. (For interpretation of the references to colour in this figure legend, the reader is referred to the web version of this article.)

Table 2
Inhibitory effect of designed compounds against SENP1.

Compound	Structure	IC ₅₀ ^a (μM)
13a		26.6
13b		9.1
13c		6.4
13d		16.4
13e		9.2
13f		4.9
13g		6.2
13h		7.6
13i		12.4
13j		7.1
13k		15.3
13l		8.5
13m		3.5
13n		8.0

^a IC₅₀ measurement has an error range within ±10%.

or Trp534, while the L¹ and L² linkages form hydrogen bond interactions. The A³ moiety points to the His533-Met552 site.

The predicted binding poses of compounds **1** and **5** are shown in Fig. 2. Both compounds assume binding poses that closely resemble the binding conformation of peptide E⁸⁸QTGGHS⁹⁴ derived from pre-SUMO. Compound **1** showed hydrogen bonds with Lys455, His529, Val532, Leu466, and Gln597, π–π interaction with Trp465, His533, and Trp534, and hydrophobic interaction with Met552. Compound **5** showed hydrogen bonds with Leu466, His529, Val532, and Gln597, π–π interaction with Trp465, His529, His533, and Trp534, and hydrophobic interaction with Phe496 and Met552.

2.3. Structural optimization and structure-activity relationship (SAR) study

In order to improve their SENP1 inhibitory activity, we designed and synthesized compounds **13a–13n** (Table 2) based on the core structural features of A¹-L¹-A²-L²-A³ which is derived from the initial hits.

We selected compounds **1** and **5** as the model compounds. Their aryl groups, phenyl and benzothio-phenyl, were incorporated as the A¹, A², and A³ groups. Their amide groups with the nitrogen atom either directly connected to or a carbon atom away from the central phenyl were incorporated as the L¹ and L² linkage groups. This resulted in the structure of compound **13a** whose SENP1 inhibitory activity (IC₅₀ = 26.6 μM) was shown to be weaker than compounds **1** and **5**. The docking structure of **13a** with SENP1 showed that the structure spans a shorter dimension than compound **1** or **5**, which might contribute to its decreased activity. After the benzothio-phenyl was replaced by a larger group, i.e. bromobiphenyl, the inhibitory activity (compound **13b**, IC₅₀ = 9.1 μM) became superior to compounds **1** and **5**. The docking structure of **13b** in SENP1 showed that the phenyl group at the A³ terminus was near the His533 and Met552 residues which potentially could form sandwiched hydrophobic interaction, and extension of the linkage group may enhance this interaction (Fig. 3). Thus, compound **13c** with an extended linkage group containing a double bond was synthesized and showed a slightly improved IC₅₀ value of 6.4 μM. The docked model showed that compound **13c** formed favorable hydrophobic interaction with His533 and Met552. Both compounds **13b** and **13c** formed four hydrogen bonds with residues Leu466, His529, Val532, and Gln597.

Next, compounds **13d–13j** with various substituents at the A¹ terminus were synthesized in order to further improve the SENP1 inhibitory activity from compound **13c**. The meta-bromo derivative **13d** showed a 2.5-fold decrease of activity (IC₅₀ = 16.4 μM). Removal of the bromo-atom gave comparable activity (**13e**, IC₅₀ = 9.2 μM). The *para*-methoxy compound **13f** showed the best potency (IC₅₀ = 4.9 μM) among the derivatives of **13c**. When the biphenyl group was replaced with various aryl rings (compounds **13g–13j**), the SENP1 inhibitory activity was not improved.

We next tested the effect of the flexibility of linkage group L² on the inhibitory activity. Compounds **13k–13n** which are the single bond derivatives of the double bond-containing compounds **13c**, **13e**, **13f**, and **13g** were synthesized. For compounds **13k**, **13l**, and **13n**, more flexibility led to either reduced or comparable activity. However, compound **13m** gave the most potent inhibitory activity (IC₅₀ = 3.5 μM) among all compounds in this work.

The synthesis of these compounds are described below. As shown in Scheme 1, aminomethylaniline was used as the common starting material. After the benzyl amino group was protected by Boc, the phenylamino group was coupled with various carboxylic acids in the presence of EDCI/DMAP followed by treatment with TFA to give compounds **12a–12c**. Compounds **13a–13n** were subsequently prepared by coupling compounds **12a–12c** with the corresponding carboxylic acids.

3. Conclusions

The SENPs which catalyze the deconjugation of SUMO from their target proteins play essential roles in a variety of critical cellular events. Dysfunction of the equilibrium of SUMOylation and deSUMOylation is associated with numerous pathological conditions including cancer. Specifically, SENP1 has been found to be closely related to the prostate and colon cancer. As a potential therapeutic target, the discovery of SENP1 inhibitors remains in its infancy. In this study, we identified 11 SENP1 inhibitors with various scaffolds through *in silico* screening. Based on the structural features and the docked poses of the initial hits, compounds **13a–13n** were designed and synthesized, which gave improved SENP1 inhibitory activity with compound **13m** (IC₅₀ = 3.5 μM) as the most potent compound in this series. We believe these new SENP1 inhibitors will contribute to the further development of SENP1 inhibitors as potential therapeutics and functional probes.

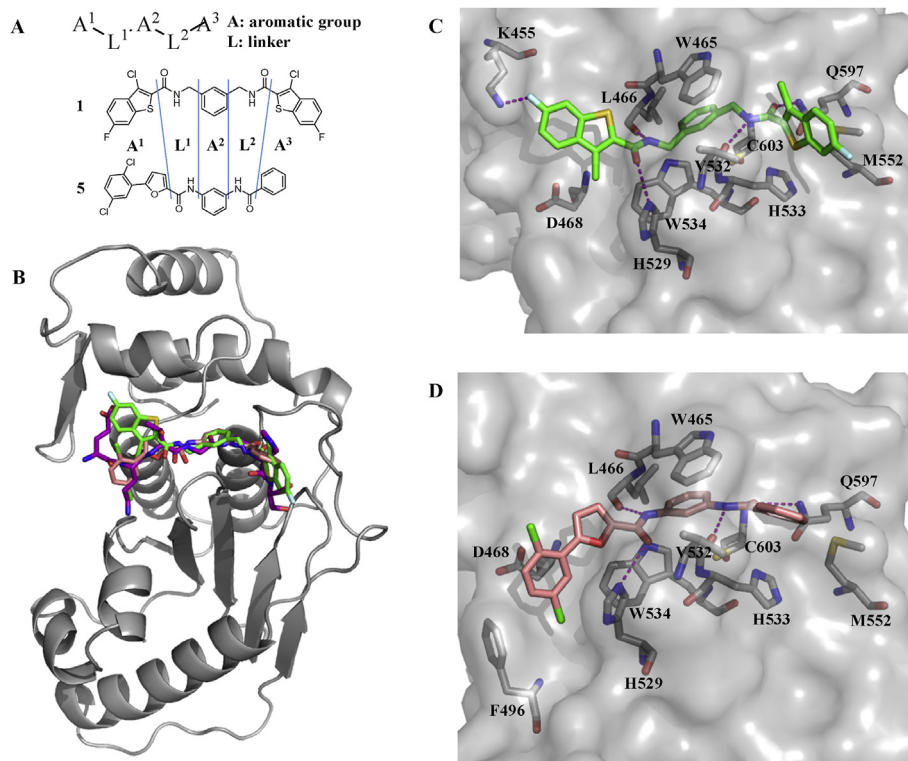


Fig. 2. A, Representative structure of SENP1 inhibitors. B, Overlap of compounds **1** (green stick), **5** (salmon stick) and E⁸⁸QTGGH⁹⁴ of pre-SUMO (purple stick) in SENP1 (gray cartoon) pocket. C, Detailed interactions between compound **1** and SENP1 (gray surface). D, Detailed interactions between compound **5** and SENP1 (gray surface). The residues interacting with compound **1** or **5** are shown in gray stick. (For interpretation of the references to colour in this figure legend, the reader is referred to the web version of this article.)

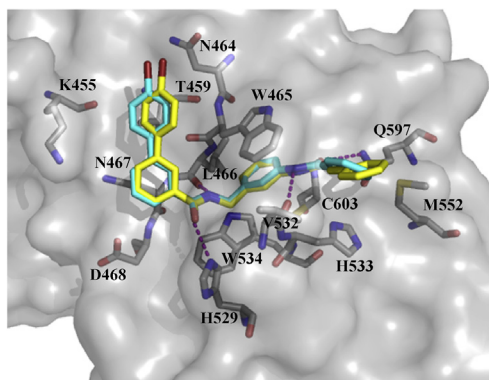
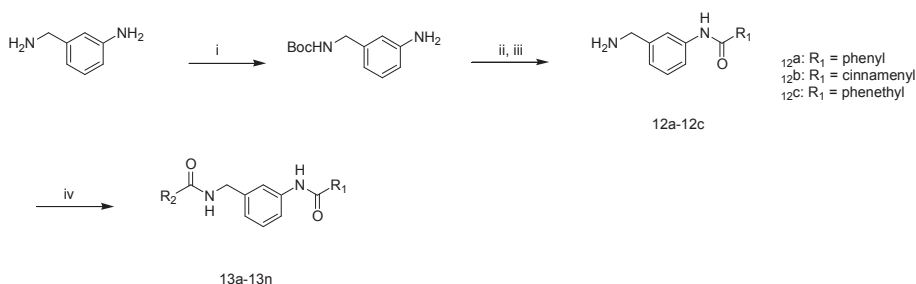


Fig. 3. Overlap of compounds **13b** (cyan stick) and **13c** (yellow stick) in SENP1 (gray surface) pocket. The residues interacting with compounds **13b** and **13c** are shown in gray stick. (For interpretation of the references to colour in this figure legend, the reader is referred to the web version of this article.)

4. Material and methods

4.1. Preparation of protein and small molecule database for computational study

The 3D structure of the SENP1-pre-SUMO complex (PDB ID: 2IY1) was used to derive the SENP1-T⁹⁰GGH⁹³ peptide complex that was used in the study and is described as follows. Using the workflows of Maestro [23], the A603 was mutated back to C603, the hydrogen atoms were added, the bond orders were assigned, the added hydrogen atoms were optimized with exhaustive sampling method, and all atoms were energy minimized to reach the convergent RMSD of 0.30 Å with the OPLS_2005 force field [24]. The docking grid was then generated using Glide 5 [25]. The centroid of the T⁹⁰GGH⁹³ peptide was defined as the active site center and the bounding box which contains the acceptable positions for the ligand center was set to 14 Å × 14 Å × 14 Å. The Specs database which includes approximately 197,000 commercially



Scheme 1. Reagents and conditions: (i) Boc₂O, TEA, DCM, rt, 20 h; (ii) R₁COOH, DCM, EDCI, DMAP, rt, overnight; (iii) TFA, DCM, rt, 2 h; (iv) R₂COOH, DCM, EDCI, DMAP, rt, overnight.

available compounds was used for *in silico* screening. LigPrep [26] was used to prepare these compounds in OPLS_2005 force field. The possible ionization state at $\text{pH} = 7.0 \pm 2.0$ was generated for each compound. About 350,000 small molecule conformations were generated.

4.2. *In silico* screening

The Glide module [25] was employed to screen the Specs database in order to identify SENP1 inhibitors. The screening was done by three consecutive flows: HTVS (350,000 compounds screened), SP (top ranked 40,000 compounds from HTVS screened), and XP (top ranked 5000 compounds from SP screened). The ligands were set to be flexible, the ring conformations were sampled, and the non-planar conformations for amide bonds were penalized. The docked conformations were ranked by Glide scoring function. Both top ranked 150 molecules after SP sieve and top ranked 150 molecules after XP sieve were manually analyzed. Finally, 30 compounds were purchased and tested.

4.3. Bioactivity assay

The pET28a-SENP1 plasmid (catalytic core, residues 419–644) was transformed into *Escherichia coli* BL21 (DE3). Expression of SENP1 was induced with 0.5 mM IPTG at 16 °C for 16 h. Cell pellets were resuspended in lysis buffer (50 mM $\text{Na}_2\text{HPO}_4/\text{NaH}_2\text{PO}_4$ pH 7.4, 300 mM NaCl, 10% glycerol, 10 mM β -mercaptoethanol, and 10 mM imidazole) and sonicated. SENP1 was purified using Ni-NTA resin (Qiagen) and eluted with elution buffer containing 150 mM imidazole. The pET28a-RanGAP (residues 403–585) and pSAE1/SAE2-UBC9-SUMO plasmids were cotransformed into *E. coli* BL21 (DE3), and similar methods were used in the expression and purification of fusion protein RanGAP-SUMO.

The SENP1 inhibitory effect of the compounds was tested using deSUMOylation assay. SENP1 (4 nM) was incubated with compounds at 37 °C for 10 min in reaction buffer (50 mM Tris-HCl pH 8.0, 20 mM NaCl, 2 mM DTT, 2 mM CaCl_2). Then 5 μL RanGAP-SUMO (2 $\mu\text{g}/\mu\text{L}$) was added and incubated for another 25 min at 37 °C. The reaction was terminated by adding loading buffer and boiling for 5 min. The protein samples were subjected to SDS-PAGE and coomassie staining. The RanGAP-SUMO bands were quantified on the Odyssey infrared scanner ($\lambda_{\text{ex}} = 680 \text{ nm}$ and $\lambda_{\text{em}} = 720 \text{ nm}$).

Percentage inhibition was calculated using the following equation: $\% \text{inhibition} = [(\text{RFU}_{\text{sample}} - \text{RFU}_{\text{blank}}) / (\text{RFU}_{\text{substrate}} - \text{RFU}_{\text{blank}})] \times 100\%$, sample - RanGAP-SUMO, SENP1, and compounds in assay buffer, blank - RanGAP-SUMO, SENP1 in assay buffer, substrate - RanGAP-SUMO in assay buffer without SENP1. For IC_{50} measurement, a test compound at interval concentrations (50, 25, 12.5, 6.25, 3.12, 1.56, 0.78, 0.39 μM) was used and the data were fitted with GraphPad to give the IC_{50} value.

4.4. Chemistry

All solvents and reagents were purchased from commercial sources and used without further purification unless otherwise noted. NMR spectra were recorded on Bruker Avance III 400 MHz or 600 MHz. Chemical shifts are expressed in parts per million (ppm) relative to residual solvent as an internal reference ($\text{DMSO}-d_6$: 2.50). High resolution mass spectra were obtained on Agilent 6530 Accurate Mass Q-TOF LC-MS. Column chromatography was performed using Huanghai silica gel (45–75 μm). HPLC analysis was performed on an Agilent 200 with a flow rate of 1 mL/min and a gradient of 10% v/v MeOH in H_2O ($t = 0 \text{ min}$) to 100% MeOH ($t = 15.0 \text{ min}$) stopping at 20 or 25 min using a DAD detector. An Agilent Eclipse XDB-C18 column (4.6 mm \times 150 mm, 5 μm) was

used. Purity was based on the integrated UV chromatogram (254 nm). The purity of all biological assay compounds was >95%.

4.4.1. *N*-[3-(Aminomethyl)phenyl]benzamide (**12a**)

The solution of EDCI (3.14 g, 16.38 mmol) and DMAP (100 mg, 0.82 mmol) in 10 mL DCM was added dropwise to a mixture of tert-butyl-3-aminobenzyl-carbamate (2.0 g, 9.01 mmol) and benzoic acid (1.0 g, 8.19 mmol) in 20 mL DCM at 0 °C under nitrogen atmosphere, and the mixture was warmed to r.t. and stirred overnight. After quenched with water and extracted with DCM, the organic layer was washed with 1 M NaOH (20 mL), 1 M HCl (20 mL), and saturated NaHCO_3 (10 mL), dried over Na_2SO_4 , and concentrated under reduced pressure. The Boc-protected **12a** was dissolved in DCM (5 mL), trifluoroacetic acid (5 mL) was added. The reaction mixture was allowed to stir for 2 h at r.t. and concentrated under reduced pressure. The residue was purified by column chromatography over silica gel and further purified by recrystallization (ethyl ether) to obtain the title compound as a white solid (1.2 g, yield 64.8%). ^1H NMR (600 MHz, $\text{DMSO}-d_6$) δ : 10.42 (1H, s), 8.34 (3H, s), 8.01–7.96 (3H, m), 7.70 (1H, d, $J = 8.4 \text{ Hz}$), 7.61 (1H, t, $J = 8.4 \text{ Hz}$), 7.54 (2H, t, $J = 7.8 \text{ Hz}$), 7.41 (1H, t, $J = 7.8 \text{ Hz}$), 7.22 (1H, d, $J = 7.8 \text{ Hz}$), 4.04 (2H, s). ^{13}C NMR (150 MHz, $\text{DMSO}-d_6$) δ : 166.1, 139.9, 135.2, 134.9, 132.1, 129.4, 128.8, 128.1, 124.4, 121.3, 121.0, 42.9.

4.4.2. *N*-[3-(Aminomethyl)phenyl]cinnamamide (**12b**)

Compound **12b** was prepared following a similar procedure to compound **12a**. Yield: 53.5%. ^1H NMR (600 MHz, $\text{DMSO}-d_6$) δ : 10.24 (1H, s), 7.67 (1H, s), 7.65–7.54 (4H, m), 7.49–7.38 (3H, m), 7.28 (1H, t, $J = 8.0 \text{ Hz}$), 7.08 (1H, d, $J = 8.0 \text{ Hz}$), 6.88 (1H, d, $J = 16 \text{ Hz}$), 3.76 (2H, s). ^{13}C NMR (150 MHz, $\text{DMSO}-d_6$) δ : 163.9, 143.6, 140.4, 139.6, 135.2, 130.2, 129.4, 129.1, 128.2, 122.9, 122.8, 118.6, 118.1, 45.6.

4.4.3. *N*-[3-(Aminomethyl)phenyl]-3-phenylpropanamide (**12c**)

Compound **12c** was prepared following a similar procedure to compound **12a**. Yield: 66.8%. ^1H NMR (600 MHz, $\text{DMSO}-d_6$) δ : 10.08 (1H, s), 8.25 (3H, s), 7.78 (1H, s), 7.48 (1H, d, $J = 8.4 \text{ Hz}$), 7.34 (1H, t, $J = 8.4 \text{ Hz}$), 7.32–7.24 (4H, m), 7.18 (1H, t, $J = 7.2 \text{ Hz}$), 7.13 (1H, d, $J = 7.8 \text{ Hz}$), 3.99 (2H, q, $J = 6.0 \text{ Hz}$), 2.91 (2H, t, $J = 7.8 \text{ Hz}$), 2.65 (2H, t, $J = 7.8 \text{ Hz}$). ^{13}C NMR (150 MHz, $\text{DMSO}-d_6$) δ : 171.0, 141.5, 139.9, 134.9, 129.5, 128.7, 128.6, 126.4, 123.8, 120.0, 119.6, 42.9, 38.2, 31.2.

4.4.4. Benzo[*b*]thiophene-2-carboxylic acid 3-benzoylamino-benzylamide (**13a**)

The solution of EDCI (107 mg, 0.56 mmol) and DMAP (3 mg, 0.03 mmol) in 5 mL DCM was added dropwise to a mixture of compound **12a** (69 mg, 0.31 mmol) and benzo[*b*]thiophene-2-carboxylic acid (50 mg, 0.28 mmol) in 5 mL DCM at 0 °C under nitrogen atmosphere, and the mixture was warmed to r.t. and stirred overnight. The mixture was quenched with water and extracted with DCM. The organic layer was washed with 1 M NaOH (20 mL), 1 M HCl (20 mL), and saturated NaHCO_3 (10 mL), dried over Na_2SO_4 , and concentrated under reduced pressure. The residue was purified by column chromatography over silica gel and further purified by recrystallization (ethyl ether) to obtain the title compound as a white solid (45 mg, yield 41.5%) Mp: 258–260 °C. ^1H NMR (400 MHz, $\text{DMSO}-d_6$) δ : 10.31 (1H, s), 9.43 (1H, t, $J = 6.0 \text{ Hz}$), 8.20 (1H, s), 8.02 (1H, d, $J = 7.2 \text{ Hz}$), 7.99–7.91 (3H, m), 7.79 (1H, s), 7.73 (1H, d, $J = 8.0 \text{ Hz}$), 7.56 (1H, m), 7.55–7.41 (4H, m), 7.33 (1H, t, $J = 8.0 \text{ Hz}$), 7.10 (1H, d, $J = 7.2 \text{ Hz}$), 4.51 (2H, d, $J = 6.0 \text{ Hz}$). ^{13}C NMR (100 MHz, $\text{DMSO}-d_6$) δ : 166.1, 161.9, 140.6, 140.4, 140.2, 139.7, 139.6, 135.3, 131.9, 129.0, 128.8, 128.1, 126.6, 125.6, 125.3, 123.3, 123.2, 119.7, 119.5, 43.2. HRMS calcd for $\text{C}_{23}\text{H}_{19}\text{N}_2\text{O}_2\text{S}$ ($\text{M}+\text{H}$)⁺ 387.1167, found 387.1164. HPLC purity: 97.4% (14.0 min).

4.4.5. 4'-Bromo-biphenyl-3-carboxylic acid 3-benzoylamino-benzylamide (**13b**)

Compound **13b** was prepared following a similar procedure to compound **13a**. Yield: 37.5%. Mp: 253–256 °C. ¹H NMR (600 MHz, DMSO-*d*₆) δ: 10.27 (1H, s), 9.22 (1H, t, *J* = 6.0 Hz), 8.22 (1H, s), 7.94 (3H, m), 7.85 (1H, d, *J* = 7.8 Hz), 7.78 (1H, s), 7.75–7.65 (5H, m), 7.62–7.55 (2H, m), 7.51 (1H, t, *J* = 7.8 Hz), 7.32 (1H, t, *J* = 7.8 Hz), 7.10 (1H, d, *J* = 7.8 Hz), 4.54 (2H, d, *J* = 6.0 Hz). ¹³C NMR (150 MHz, DMSO-*d*₆) δ: 166.4, 166.0, 140.6, 139.7, 139.4, 139.4, 135.6, 135.4, 132.3, 132.0, 129.8, 129.6, 129.4, 129.0, 128.8, 128.1, 127.4, 125.7, 123.1, 121.8, 119.5, 119.3, 43.2. HRMS calcd for C₂₇H₂₂N₂O₂Br (M+H)⁺ 485.0865, found 385.0861. HPLC purity: 95.7% (15.7 min).

4.4.6. 4'-Bromo-biphenyl-3-carboxylic acid 3-(3-phenyl-acryloylamino)-benzylamide (**13c**)

The solution of EDCI (107 mg, 0.56 mmol) and DMAP (3 mg, 0.03 mmol) in 5 mL dichloromethane was added dropwise to a mixture of compound **12b** (78 mg, 0.31 mmol) and 4'-bromo-biphenyl-3-carboxylic acid (50 mg, 0.18 mmol) in 5 mL DCM at 0 °C under nitrogen atmosphere, and the mixture was warmed to r.t. and stirred overnight. After quenched with water and extracted with DCM, the organic layer was washed with 1 M NaOH (20 mL), 1 M HCl (20 mL), and saturated NaHCO₃ (10 mL), dried over Na₂SO₄, and concentrated under reduced pressure. The residue was purified by column chromatography over silica gel and further purified by recrystallization (ethyl ether) to obtain the title compound as a white solid (43 mg, yield 30.3%). Mp: 236–238 °C. ¹H NMR (400 MHz, DMSO-*d*₆) δ: 10.21 (1H, s), 9.23 (1H, t, *J* = 6.0 Hz), 8.23 (1H, s), 7.99 (1H, s), 7.95 (1H, d, *J* = 8.0 Hz), 7.89 (1H, d, *J* = 8.0 Hz), 7.78 (1H, d, *J* = 7.6 Hz), 7.71–7.53 (7H, m), 7.51–7.38 (4H, m), 7.31 (1H, t, *J* = 7.6 Hz), 7.07 (1H, d, *J* = 7.6 Hz), 6.83 (1H, d, *J* = 15.6 Hz), 4.54 (2H, d, *J* = 6.0 Hz). ¹³C NMR (100 MHz, DMSO-*d*₆) δ: 166.4, 163.9, 140.8, 140.6, 139.8, 139.4, 139.4, 135.5, 135.2, 132.3, 132.0, 130.3, 129.8, 129.7, 129.5, 129.4, 129.2, 128.2, 127.4, 125.7, 122.8, 121.8, 118.2, 118.2, 43.1. HRMS calcd for C₂₉H₂₄N₂O₂Br (M+H)⁺ 511.1021, found 511.1021. HPLC purity: 98.7% (13.8 min).

4.4.7. 3'-Bromo-biphenyl-3-carboxylic acid 3-(3-phenyl-acryloylamino)-benzylamide (**13d**)

Compound **13d** was prepared following a similar procedure to compound **13c**. Yield: 47.4%. Mp: 231–233 °C. ¹H NMR (400 MHz, DMSO-*d*₆) δ: 10.21 (1H, s), 9.24 (1H, t, *J* = 6.0 Hz), 8.24 (1H, s), 7.94 (1H, d, *J* = 8.0 Hz), 7.86 (1H, d, *J* = 8.0 Hz), 7.77–7.65 (6H, m), 7.64–7.57 (4H, m), 7.48–7.38 (3H, m), 7.31 (1H, t, *J* = 7.6 Hz), 7.07 (1H, d, *J* = 7.6 Hz), 6.84 (1H, d, *J* = 15.6 Hz), 4.54 (2H, d, *J* = 6.0 Hz). ¹³C NMR (100 MHz, DMSO-*d*₆) δ: 166.4, 163.9, 142.4, 140.7, 140.6, 139.8, 139.1, 135.5, 135.2, 131.6, 131.0, 130.2, 130.1, 129.9, 129.7, 129.5, 129.0, 129.2, 128.2, 127.8, 126.5, 125.9, 122.9, 122.8, 118.2, 118.2, 43.1. HRMS calcd for C₂₉H₂₄N₂O₂Br (M+H)⁺ 511.1021, found 511.1026. HPLC purity: 97.4% (15.1 min).

4.4.8. Biphenyl-3-carboxylic acid 3-(3-phenyl-acryloylamino)-benzylamide (**13e**)

Compound **13e** was prepared following a similar procedure to compound **13c**. Yield: 49.4%. Mp: 191–193 °C. ¹H NMR (400 MHz, DMSO-*d*₆) δ: 10.21 (1H, s), 9.23 (1H, t, *J* = 6.0 Hz), 8.23 (1H, s), 7.92 (1H, d, *J* = 8.0 Hz), 7.86 (1H, d, *J* = 7.6 Hz), 7.77 (2H, d, *J* = 7.2 Hz), 7.68 (1H, d, *J* = 8.0 Hz), 7.66–7.54 (5H, m), 7.51 (2H, t, *J* = 7.6 Hz), 7.48–7.38 (4H, m), 7.31 (1H, t, *J* = 7.6 Hz), 7.06 (1H, d, *J* = 7.6 Hz), 6.83 (1H, d, *J* = 15.6 Hz), 4.53 (2H, d, *J* = 6.0 Hz). ¹³C NMR (100 MHz, DMSO-*d*₆) δ: 166.5, 164.0, 140.9, 140.7, 140.6, 140.0, 139.9, 135.4, 135.2, 130.2, 129.9, 129.6, 129.5, 129.2, 128.3, 128.2, 127.4, 127.0, 125.9, 122.8, 118.3, 118.2, 43.1. HRMS calcd for C₂₉H₂₅N₂O₂ (M+H)⁺ 433.1916, found 433.1914. HPLC purity: 98.1% (15.0 min).

4.4.9. 4'-Methoxy-biphenyl-3-carboxylic acid 3-(3-phenyl-acryloylamino)-benzylamide (**13f**)

Compound **13f** was prepared following a similar procedure to compound **13c**. Yield: 30.8%. Mp: 195–197 °C. ¹H NMR (400 MHz, DMSO-*d*₆) δ: 10.22 (1H, s), 9.21 (1H, t, *J* = 6.0 Hz), 8.19 (1H, s), 7.86 (1H, d, *J* = 7.6 Hz), 7.80 (1H, d, *J* = 8.0 Hz), 7.74–7.64 (4H, m), 7.64–7.52 (4H, m), 7.48–7.38 (3H, m), 7.31 (1H, t, *J* = 7.6 Hz), 7.09–7.04 (3H, m), 6.84 (1H, d, *J* = 16 Hz), 4.53 (2H, d, *J* = 6.0 Hz), 3.81 (3H, s). ¹³C NMR (100 MHz, DMSO-*d*₆) δ: 166.6, 163.9, 159.6, 140.8, 140.5, 140.3, 139.8, 135.3, 135.1, 132.3, 130.2, 129.4, 129.3, 129.2, 128.4, 128.1, 126.2, 125.3, 122.7, 118.2, 114.8, 55.6, 43.1. HRMS calcd for C₃₀H₂₇N₂O₃ (M+H)⁺ 463.2022, found 463.2021. HPLC purity: 99.1% (15.4 min).

4.4.10. 3-Benzyloxy-N-[3-(3-phenyl-acryloylamino)-benzyl]-benzamide (**13g**)

Compound **13g** was prepared following a similar procedure to compound **13c**. Yield: 22.1%. Mp: 206–208 °C. ¹H NMR (400 MHz, DMSO-*d*₆) δ: 10.22 (1H, s), 9.07 (1H, t, *J* = 6.0 Hz), 7.66 (1H, d, *J* = 8.0 Hz), 7.64–7.54 (5H, m), 7.52 (1H, d, *J* = 8.0 Hz), 7.50–7.38 (8H, m), 7.37–7.27 (2H, m), 7.19 (1H, dd, *J* = 8.0, 2.0 Hz), 7.03 (1H, d, *J* = 8.0 Hz), 6.84 (1H, d, *J* = 15.6 Hz), 5.17 (2H, s), 4.48 (2H, d, *J* = 6.0 Hz). ¹³C NMR (100 MHz, DMSO-*d*₆) δ: 166.4, 164.0, 159.8, 140.8, 140.5, 139.8, 137.3, 135.2, 130.2, 129.9, 129.5, 129.1, 128.9, 128.3, 128.1, 122.8, 122.7, 120.3, 118.4, 118.3, 118.2, 114.1, 69.9, 43.1. HRMS calcd for C₃₀H₂₇N₂O₃ (M+H)⁺ 463.2022, found 463.2021. HPLC purity: 99.5% (15.4 min).

4.4.11. N-(3-Cinnamidobenzyl)-2-naphthamide (**13h**)

Compound **13h** was prepared following a similar procedure to compound **13c**. Yield: 25.9%. Mp: 215–216 °C. ¹H NMR (400 MHz, DMSO-*d*₆) δ: 10.21 (1H, s), 9.25 (1H, t, *J* = 6.0 Hz), 8.54 (1H, s), 8.07–7.98 (4H, m), 7.68 (1H, d, *J* = 8.0 Hz), 7.65 (1H, s), 7.64–7.54 (5H, m), 7.48–7.38 (3H, m), 7.31 (1H, t, *J* = 7.6 Hz), 7.09 (1H, d, *J* = 7.6 Hz), 6.83 (1H, d, *J* = 15.6 Hz), 4.55 (2H, d, *J* = 6.0 Hz). ¹³C NMR (100 MHz, DMSO-*d*₆) δ: 166.7, 163.9, 140.8, 140.5, 139.8, 135.2, 134.6, 132.6, 130.2, 129.5, 129.3, 129.2, 128.4, 128.2, 128.1, 128.0, 127.2, 124.6, 122.8, 122.7, 118.3, 118.2, 43.2. HRMS calcd for C₂₇H₂₃N₂O₂ (M+H)⁺ 407.1760, found 407.1764. HPLC purity: 98.5% (14.8 min).

4.4.12. (E)-N-(3-Cinnamidobenzyl)-1-naphthamide (**13i**)

Compound **13i** was prepared following a similar procedure to compound **13c**. Yield: 26.7%. Mp: 210–212 °C. ¹H NMR (400 MHz, DMSO-*d*₆) δ: 10.26 (1H, s), 9.12 (1H, t, *J* = 6.0 Hz), 8.26 (1H, m), 8.04 (1H, d, *J* = 8.4 Hz), 7.98 (1H, m), 7.77 (1H, s), 7.73–7.54 (8H, m), 7.48–7.38 (3H, m), 7.34 (1H, t, *J* = 7.6 Hz), 7.12 (1H, d, *J* = 7.6 Hz), 6.87 (1H, d, *J* = 15.6 Hz), 4.55 (2H, d, *J* = 6.0 Hz). ¹³C NMR (100 MHz, DMSO-*d*₆) δ: 169.1, 164.0, 140.8, 140.6, 139.9, 135.2, 135.1, 133.6, 130.3, 130.3, 130.3, 129.5, 129.3, 128.7, 128.2, 127.2, 126.7, 125.9, 125.7, 125.5, 122.8, 118.4, 118.2, 43.0. HRMS calcd for C₂₇H₂₃N₂O₂ (M+H)⁺ 407.1760, found 407.1763. HPLC purity: 95.9% (14.8 min).

4.4.13. Benzo[b]thiophene-2-carboxylic acid 3-(3-phenyl-acryloylamino)-benzylamide (**13j**)

Compound **13j** was prepared following a similar procedure to compound **13c**. Yield: 34.6%. Mp: 163–165 °C. ¹H NMR (400 MHz, DMSO-*d*₆) δ: 10.24 (1H, s), 9.37 (1H, t, *J* = 6.0 Hz), 8.17 (1H, s), 8.04 (1H, d, *J* = 7.2 Hz), 7.96 (1H, dd, *J* = 6.4, 2.0 Hz), 7.68 (1H, d, *J* = 8.0 Hz), 7.65 (1H, s), 7.63–7.54 (3H, m), 7.51–7.38 (5H, m), 7.32 (1H, t, *J* = 7.6 Hz), 7.06 (1H, d, *J* = 7.6 Hz), 6.84 (1H, d, *J* = 15.6 Hz), 4.50 (2H, d, *J* = 6.0 Hz). ¹³C NMR (100 MHz, DMSO-*d*₆) δ: 164.0, 162.0, 140.7, 140.6, 140.4, 140.3, 139.9, 139.6, 135.2, 130.2, 129.4, 129.3, 128.2, 126.7, 125.6, 125.4, 125.3, 123.3, 122.9, 122.8, 118.4, 118.3, 43.2. HRMS calcd for C₂₅H₂₁N₂O₂S (M+H)⁺ 413.1324, found 413.1324. HPLC purity: 99.5% (14.5 min).

4.4.14. 4'-Bromo-biphenyl-3-carboxylic acid 3-(3-phenyl-propionylamino)-benzylamide (**13k**)

Compound **13k** was prepared following a similar procedure to compound **13c**. Yield: 37.2%. Mp: 191–193 °C. ¹H NMR (400 MHz, DMSO-*d*₆) δ: 9.90 (1H, s), 9.19 (1H, t, *J* = 6.0 Hz), 8.21 (1H, s), 7.92 (1H, d, *J* = 7.6 Hz), 7.86 (1H, d, *J* = 8.0 Hz), 7.73 (2H, d, *J* = 8.4 Hz), 7.69 (2H, d, *J* = 8.4 Hz), 7.59 (1H, t, *J* = 8.0 Hz), 7.52 (2H, d, *J* = 7.2 Hz), 7.29–7.22 (5H, m), 7.16 (1H, t, *J* = 7.2 Hz), 7.01 (1H, d, *J* = 7.2 Hz), 4.49 (2H, d, *J* = 6.0 Hz), 2.89 (2H, t, *J* = 7.2 Hz), 2.60 (2H, t, *J* = 7.2 Hz). ¹³C NMR (100 MHz, DMSO-*d*₆) δ: 170.8, 166.4, 141.7, 140.6, 139.8, 139.2, 135.5, 132.4, 129.8, 129.7, 129.4, 129.1, 128.8, 128.7, 127.4, 126.4, 125.7, 122.4, 121.8, 118.2, 118.0, 43.1, 38.4, 31.3. HRMS calcd for C₂₉H₂₆BrN₂O₂ (M+H)⁺ 513.1178, found 513.1174. HPLC purity: 99.2% (15.6 min).

4.4.15. Biphenyl-3-carboxylic acid 3-(3-phenyl-propionylamino)-benzylamide (**13l**)

Compound **13l** was prepared following a similar procedure to compound **13k**. Yield: 30.1%. Mp: 159–161 °C. ¹H NMR (400 MHz, DMSO-*d*₆) δ: 9.9 (1H, s), 9.18 (1H, t, *J* = 6.0 Hz), 8.21 (1H, s), 7.9 (1H, d, *J* = 8.0 Hz), 7.85 (1H, d, *J* = 8.0 Hz), 7.76 (2H, d, *J* = 7.2 Hz), 7.58 (1H, t, *J* = 8.0 Hz), 7.55–7.48 (4H, m), 7.41 (1H, t, *J* = 7.6 Hz), 7.3–7.21 (5H, m), 7.16 (1H, td, *J* = 7.6, 1.6 Hz), 7.01 (1H, d, *J* = 7.6 Hz), 4.49 (2H, d, *J* = 6.0 Hz), 2.89 (2H, t, *J* = 7.6 Hz), 2.60 (2H, t, *J* = 7.6 Hz). ¹³C NMR (100 MHz, DMSO-*d*₆) δ: 166.7, 163.9, 140.8, 140.6, 139.8, 135.1, 134.6, 132.6, 130.2, 129.5, 129.3, 129.2, 128.4, 128.2, 128.1, 128.0, 127.2, 124.6, 122.8, 122.7, 118.3, 118.2, 43.2. HRMS calcd for C₂₉H₂₇N₂O₂ (M+H)⁺ 435.2073, found 435.2069. HPLC purity: 97.3% (15.3 min).

4.4.16. 4'-Methoxy-biphenyl-3-carboxylic acid 3-(3-phenyl-propionylamino)-benzylamide (**13m**)

Compound **13m** was prepared following a similar procedure to compound **13c**. Yield: 37.2%. Mp: 195–197 °C. ¹H NMR (400 MHz, DMSO-*d*₆) δ: 9.90 (1H, s), 9.16 (1H, t, *J* = 5.6 Hz), 8.16 (1H, s), 7.84 (1H, d, *J* = 7.2 Hz), 7.80 (1H, d, *J* = 7.6 Hz), 7.70 (2H, d, *J* = 8.4 Hz), 7.56–7.52 (3H, m), 7.29–7.23 (5H, m), 7.16 (1H, s), 7.10 (2H, d, *J* = 8.4 Hz), 7.01 (1H, d, *J* = 7.2 Hz), 4.48 (2H, d, *J* = 5.6 Hz), 3.81 (3H, s), 2.89 (2H, t, *J* = 8.0 Hz), 2.60 (2H, t, *J* = 8.0 Hz). ¹³C NMR (100 MHz, DMSO-*d*₆) δ: 170.8, 166.6, 159.6, 141.7, 140.7, 139.8, 135.4, 132.4, 129.4, 129.4, 129.1, 128.8, 128.7, 128.5, 126.4, 126.3, 125.3, 122.4, 118.2, 118.0, 114.9, 55.7, 43.1, 38.4, 31.3. HRMS calcd for C₃₀H₂₉N₂O₃ (M+H)⁺ 465.2178, found 465.2177. HPLC purity: 99.2% (15.6 min).

4.4.17. 3-Benzoyloxy-N-[3-(3-phenyl-propionylamino)-benzyl]-benzamide (**13n**)

Compound **13n** was prepared following a similar procedure to compound **13c**. Yield: 24.7%. Mp: 175–177 °C. ¹H NMR (400 MHz, DMSO-*d*₆) δ: 9.88 (1H, s), 9.02 (1H, t, *J* = 6.0 Hz), 7.55–7.54 (1H, m), 7.51–7.46 (4H, m), 7.45 (1H, s), 7.41–7.36 (3H, m), 7.34–7.31 (1H, m), 7.27–7.20 (5H, m), 7.18–7.13 (2H, m), 6.96 (1H, d, *J* = 8.0 Hz), 6.15 (1H, s), 4.42 (2H, d, *J* = 6.0 Hz), 2.88 (2H, t, *J* = 7.6 Hz), 2.58 (2H, t, *J* = 7.6 Hz). ¹³C NMR (100 MHz, DMSO-*d*₆) δ: 170.8, 166.3, 158.8, 141.7, 140.7, 139.8, 137.4, 136.3, 130.0, 129.1, 128.9, 128.8, 128.7, 128.4, 128.2, 126.4, 122.4, 120.2, 118.3, 118.2, 118.0, 114.0, 69.9, 43.1, 38.4, 31.3. HRMS calcd for C₃₀H₂₉N₂O₃ (M+H)⁺ 465.2178, found 465.2181. HPLC purity: 96.3% (15.1 min).

Acknowledgements

We thank National Science Foundation of China (81222042 and 81573264), the Ministry of Science and Technology of China (2012CB518001), the Young Teacher Start Plan of SJTU (14X100040051),

and the E-Institutes of Shanghai Universities (EISU) Chemical Biology Division (E-Institutes of Shanghai Municipal Education Commission Project E09013) for financial support of this work. We thank Prof. Yingli Wu (SJTU) for his generous provision of plasmids of pET28a-SEN1, pET28a-RanGAP and pSAE1/SAE2-UBC9-SUMO1.

Appendix A. Supplementary data

Supplementary data related to this article can be found at <http://dx.doi.org/10.1016/j.ejmech.2016.06.018>.

References

- [1] S. Martin, K.A. Wilkinson, A. Nishimune, J.M. Henley, Emerging extranuclear roles of protein SUMOylation in neuronal function and dysfunction, *Nat. Rev. Neurosci.* 8 (2007) 948–959.
- [2] P. Heun, SUMO organization of the nucleus, *Curr. Opin. Cell Biol.* 19 (2007) 350–355.
- [3] R.J. Dohmen, SUMO protein modification, *Biochim. Biophys. Acta* 1695 (2004) 113–131.
- [4] E.S. Johnson, Protein modification by SUMO, *Annu. Rev. Biochem.* 73 (2004) 355–382.
- [5] F. Melchior, M. Schergaut, A. Pichler, SUMO: ligases, isopeptidases and nuclear pores, *Trends Biochem. Sci.* 28 (2003) 612–618.
- [6] J. Zhao, Sumoylation regulates diverse biological processes, *Cell. Mol. Life Sci.* 64 (2007) 3017–3033.
- [7] R. Geiss-Friedlander, F. Melchior, Concepts in sumoylation: a decade on, *Nat. Rev. Mol. Cell Biol.* 8 (2007) 947–956.
- [8] R.T. Hay, SUMO-specific proteases: a twist in the tail, *Trends Cell Biol.* 17 (2007) 370–376.
- [9] D. Mukhopadhyay, M. Dasso, Modification in reverse: the SUMO proteases, *Trends Biochem. Sci.* 32 (2007) 286–295.
- [10] J.H. Kim, S.H. Baek, Emerging roles of desumoylating enzymes, *Biochim. Biophys. Acta* 1792 (2009) 155–162.
- [11] J. Cheng, T. Bawa, P. Lee, L. Gong, E.T. Yeh, Role of desumoylation in the development of prostate cancer, *Neoplasia* 8 (2006) 667–676.
- [12] T. Bawa-Khalife, J. Cheng, S.H. Lin, M.M. Ittmann, E.T. Yeh, SENP1 induces prostatic intraepithelial neoplasia through multiple mechanisms, *J. Biol. Chem.* 285 (2010) 25859–25866.
- [13] Y. Zuo, J.K. Cheng, Small ubiquitin-like modifier protein-specific protease 1 and prostate cancer, *Asian J. Androl.* 11 (2009) 36–38.
- [14] Y. Xu, J. Li, Y. Zuo, J. Deng, L.S. Wang, G.Q. Chen, SUMO-specific protease 1 regulates the in vitro and in vivo growth of colon cancer cells with the upregulated expression of CDK inhibitors, *Cancer Lett.* 309 (2011) 78–84.
- [15] J. Cheng, X. Kang, S. Zhang, E.T. Yeh, SUMO-specific protease 1 is essential for stabilization of HIF1α during hypoxia, *Cell* 131 (2007) 584–595.
- [16] Y. Xu, Y. Zuo, H. Zhang, X. Kang, F. Yue, Z. Yi, M. Liu, E.T. Yeh, G. Chen, J. Cheng, Induction of SENP1 in endothelial cells contributes to hypoxia-driven VEGF expression and angiogenesis, *J. Biol. Chem.* 285 (2010) 36682–36688.
- [17] Z. Qiao, W. Wang, L. Wang, D. Wen, Y. Zhao, Q. Wang, Q. Meng, G. Chen, Y. Wu, H. Zhou, Design, synthesis, and biological evaluation of benzodiazepine-based SUMO-specific protease 1 inhibitors, *Bioorg. Med. Chem. Lett.* 21 (2011) 6389–6392.
- [18] V.E. Albrow, E.L. Ponder, D. Fasci, M. Bekes, E. Deu, G.S. Salvesen, M. Bogoy, Development of small molecule inhibitors and probes of human SUMO deconjugating proteases, *Chem. Biol.* 18 (2011) 722–732.
- [19] Y. Chen, D. Wen, Z. Huang, M. Huang, Y. Luo, B. Liu, H. Lu, Y. Wu, Y. Peng, J. Zhang, 2-(4-Chlorophenyl)-2-oxoethyl 4-benzamidobenzoate derivatives, a novel class of SENP1 inhibitors: virtual screening, synthesis and biological evaluation, *Bioorg. Med. Chem. Lett.* 22 (2012) 6867–6870.
- [20] I.G. Madu, A.T. Namanja, Y. Su, S. Wong, Y.J. Li, Y. Chen, Identification and characterization of a new chemotype of noncovalent SENP inhibitors, *ACS Chem. Biol.* 8 (2013) 1435–1441.
- [21] L. Shen, M.H. Tatham, C. Dong, A. Zagorska, J.H. Naismith, R.T. Hay, SUMO protease SENP1 induces isomerization of the scissile peptide bond, *Nat. Struct. Mol. Biol.* 13 (2006) 1069–1077.
- [22] L.N. Shen, C. Dong, H. Liu, J.H. Naismith, R.T. Hay, The structure of SENP1-SUMO-2 complex suggests a structural basis for discrimination between SUMO paralogues during processing, *Biochem. J.* 397 (2006) 279–288.
- [23] Schrödinger, Maestro, Version 8.5, LLC, New York, NY, 2008.
- [24] G.A. Kaminski, R.A. Friesner, J. Tirado-Rives, W.L. Jorgensen, Evaluation and reparametrization of the OPLS-AA force field for proteins via comparison with accurate quantum chemical calculations on peptides, *J. Phys. Chem. B* 105 (2001) 6474–6487.
- [25] Schrödinger, Glide, Version 5.0, LLC, New York, NY, 2008.
- [26] Schrödinger, LigPrep, Version 2.2, LLC, New York, NY, 2005.